

Comparison of Windowed-Decoder Configurations for Spatially Coupled LDPC Codes Under Equal-Complexity Constraints

Janik Frenzel, M.Sc.^a, Dr.-Ing. Stefan Müller-Weinfurtner^b, Dr.-Ing. Johannes Huber^c, Dr.-Ing. Ralf Müller^c

^aIntel, Südwestpark 2–4, 90449, Nürnberg, Germany

^bCisco, Nordostpark 12, 90411 Nürnberg, Germany

^cFriedrich-Alexander-Universität Erlangen-Nürnberg, Digital Communications, Cauerstr. 7, 91058 Erlangen

Abstract

Spatially Coupled Low-Density Parity-Check (SC-LDPC) codes offer excellent decoding performance and can be elegantly decoded with a Windowed Decoder (WD). We determine an efficient WD configuration with low control overhead. For fair comparisons, we normalize all configurations to the same maximal computational complexity, which is an important measure of the decoding effort in packet-based data communication systems. We determine an optimized configuration from a joint evaluation of the window size, the window update strategy, and parity check-based Early Termination (ET). Firstly, we use a variable node-centered update strategy, which omits updates of messages in some parts of the decoding window. With the complexity normalization, the window size can be increased compared to a check node-centered update strategy, which uniformly updates all messages in the decoding window. Secondly, we only require the satisfaction of the top-most parity-check equations in each window to move to the next position more quickly. Using a surprisingly large window size, the resulting WD halves the average decoding complexity of the block decoder while maintaining a rather small gap in the decoding performance.

Keywords: LDPC codes, spatially coupled codes, windowed decoding, complexity constraints

1. Introduction

Spatially-Coupled (SC) Low-Density Parity-Check (LDPC) codes with Quasi-Cyclic (QC) properties [1, 2] present an appealing alternative to LDPC block codes because of their compact representation and excellent performance: A single SC-LDPC code ensemble can universally achieve the capacity of a wide range of channels [3].

There are decoder designs in literature that are more adapted to the convolutional structure of SC-LDPC codes than a Full Block Decoder (FBD), which treats the code as a block code. On the one hand, a *pipeline decoder* can utilize multiple processors to perform successive iterations on different subsets of the code's Tanner graph [1]. On the other hand, a *Windowed Decoder* (WD)—also called *sliding-window decoder*—uses a single processor to perform multiple iterations on the same subset of the graph [4, 5]. When reliability conditions are fulfilled or a maximal number of iterations is exhausted, the window slides to the next position. The decoding process resumes with some new information as windows at two successive positions overlap to a large extent.

We assume strict resource constraints to target low-power Application-Specific Integrated Circuit (ASIC) implementations and thus prefer the single-instance WD over the pipeline decoder. Additionally, the WD has two inherent advantages over the FBD: Firstly, the required amount of memory—which is typically rather expensive in ASIC designs—is greatly reduced. Secondly, the special structure of SC-LDPC codes makes it possible to detect decoding errors at an early stage. As the decoding window usually moves unidirectionally, no further message updates are scheduled in parts of the Tanner graph that have already been processed by the decoder. Residual decoding errors in the related code symbols cannot be corrected afterwards. Alternatively, there exist proposals on special WD designs where the decoding window moves bidirectionally to prevent the decoder from getting stuck [6, 7]. However, these designs require additional control loops and are not further considered in this paper.

With the restrictions to unidirectional decoding and low-overhead procedures to simplify hardware implementations, there remain three major aspects that determine the decoding performance and the computational complexity of a WD: Firstly, the *size of the decoding window* to control the amount of information processed at once. Secondly,

the *update strategy* within the window to control which parts of the decoding window are updated. Thirdly, *Early Termination* (ET) to stop the decoding before a maximal number of iterations is exhausted, thereby reducing the computational complexity.

One update strategy is to specify the window by a set of Variable Nodes (VNs) that are updated [4, 8, 9]. However, some VNs within a window then share Check Nodes (CNs) with VNs that have already moved out of that window. Messages sent along the corresponding edges are not updated any longer, i.e., they are read-only. There exist proposals on overcoming this potential drawback, e.g., by applying some form of amplification to these read-only messages [10]. A different update strategy inherently avoids this issue by defining the window by a set of CNs that are updated [5, 11]. With this strategy, messages sent along all edges connected to the involved CNs receive updates, including the messages omitted in the previously described update strategy. This CN-centered procedure nicely matches CN-wise serial update schedules that generate all outgoing messages from a CN at the same time and do so one CN after the other [12]. Such update schedules work well with the Min-Sum Algorithm (MSA) typically implemented in practice since the minimum must be found across all messages directed towards each CN [13]. Still, we also evaluate the VN-centered procedure with CN-wise serial update schedules for reasons of fairness.

For ET, there again exist at least two distinct approaches. Many criteria in literature are based on code symbol reliabilities [9, 14]. Alternatively, the Parity-Check (PC) equations inherent to SC-LDPC codes can be used for ET just as for LDPC block codes: The decoding window moves to the next position as soon as all PC equations in the window are fulfilled [4]. We favor PC-based criteria because the most recent PC results are implicitly contained in the signs of the messages exchanged during iterative decoding when using Log-Likelihood Ratios (LLRs) and CN-wise update scheduling. Hence, there is no computational overhead as the soft-value processing required for the LLRs, e.g., combination of multiples values and comparisons against a threshold, can be omitted. Still, the question remains whether *all* PC equations in the window should be considered for ET or just a subset of them. Although partial evaluations are proposed in [6, 15], to our best knowledge no evaluation of the computational complexity for soft-input soft-output decoding is available so far.

In sum, a WD can be configured in different ways than an FBD. Still, to our best knowledge, no holistic evaluation of the window size, window update strategies, and PC-based ET is available in literature so far. We try to fill this gap by performing comparisons in terms of the decoding performance and, more importantly, the resulting computational complexity. The goal of this paper is to compare configurations of a WD to find a low-complexity configuration with minimal control overhead. We find that the decoding performance of a WD with the configuration determined in this paper is not far off from that of the an FBD while resulting in a significantly reduced computational complexity.

Lastly, we use terminated codes—which are used in practical systems—instead of continuous encoding and decoding. The termination also results in a superior decoding performance [16]. We furthermore assume the use case of data packets, which usually requires all information symbols to be correctly estimated before further processing by higher layers of the communication protocol takes place. Thus, we ignore the inherent advantage in decoding latency a WD has compared to an FBD. We rather consider the time or effort it takes to decode all information symbols to measure the decoding complexity. Consequently, we limit all decoding schemes evaluated in this paper to the (approximately) same maximal number of updates of messages along the edges in the Tanner graph of the code.

The remainder of this paper is structured as follows: Section 2 summarizes SC-LDPC codes and iterative message-passing algorithms; Section 3 reviews WD configurations. The setup for numerical results is listed in Section 4. Numerical decoding results are presented in Section 5. The paper concludes with Section 6.

2. Background

This section briefly recapitulates SC-LDPC codes with QC properties and the principle of iterative decoding using message-passing algorithms. Even though only a particular set of codes is used in this paper, the concepts discussed in Section 3 are not restricted to this special code design.

2.1. Spatially-Coupled Quasi-Cyclic LDPC Codes

We use asymptotically regular SC-LDPC codes with QC properties [17]. QC codes offer a variety of benefits, namely compact representation and great potential for parallelization [18]. Together with the sparseness of LDPC codes enabling efficient encoding and iterative decoding, these beneficial properties are the reason QC-LDPC codes

are used in several applications, e.g., the 5G New Radio (NR) cellular-communications standard [19]. Although QC-LDPC codes have originally been introduced by *copy-and-permute* operations on graphs [20], we prefer the matrix notation used in, e.g., [21]. Throughout this paper, bold symbols indicate vectors (noncapitalized letters) or matrices (capitalized letters).

2.1.1. Quasi-Cyclic Low-Density Parity-Check Codes

The binary Parity-Check Matrix (PCM) \mathbf{H} of a QC-LDPC code is constructed by *lifting* an *exponent matrix* \mathbf{E} of size $M \times N$ where M and N denote the number of blocks of CNs and VNs in \mathbf{H} , respectively. With \mathbb{Z} denoting the set of integers and $\mathbb{F}_2 = \{0, 1\}$ denoting the binary field, we write

$$\mathcal{L} : \mathbf{E} \in \mathbb{Z}^{M \times N} \mapsto \mathbf{H} \in \mathbb{F}_2^{MQ \times NQ}. \quad (1)$$

Each element E_{ji} of \mathbf{E} , $j = 0 \dots (M-1)$, $i = 0 \dots (N-1)$, denotes a *cyclic shift*. The lifting operation \mathcal{L} replaces the cyclic shifts E_{ji} by square matrices of size $Q \times Q$ where Q is the *lifting factor*. If $E_{ji} \geq 0$, the substituted matrix is an identity matrix that has its rows circularly rotated to the right E_{ji} times.¹ Otherwise, the substituted matrix is an all-zero matrix. The resulting PCM \mathbf{H} of the binary $(n, m-n)$ LDPC code thus has $m = MQ$ rows and $n = NQ$ columns. Each $Q \times Q$ sub-matrix corresponds to Q consecutive CNs and VNs, forming the respective CN and VN *blocks*.

2.1.2. Terminated QC-SC-LDPC Codes

Instead of transmitting codewords individually with respect to the exponent matrix \mathbf{E} , several codewords can be *spatially coupled*. Thereby, a structure similar to convolutional codes is obtained [8]. The resulting code with memory m_s is described by exponent matrices $\mathbf{E}_\mu(t)$ with $\mu = 0 \dots m_s$ that define *sub-codes*. The argument t denotes the time index for possibly time-varying sub-codes. The $\mathbf{E}_\mu(t)$ have size $M_s \times N_s$ each, i.e., N_s blocks of code bits are transmitted at each time index, forming M_s blocks of PC equations. For a code with memory m_s , up to $m_s + 1$ sub-codes $\mathbf{E}_\mu(t)$ influence each encoded code bit. The length of the entire code is defined by the *coupling length* L . As argued above, we focus on terminated codes and thus use a finite coupling length. The entire exponent matrix $\mathbf{E}_{[0,L-1]}$ of a terminated SC-LDPC code with coupling length L has $M = M_s(L + m_s)$ rows and $N = N_s L$ columns and is described by

$$\mathbf{E}_{[0,L-1]} = \begin{bmatrix} \mathbf{E}_0(0) & & & \\ \vdots & \ddots & & \\ \mathbf{E}_{m_s}(m_s) & \ddots & \mathbf{E}_0(L-1) & \\ & \ddots & \vdots & \\ & & \mathbf{E}_{m_s}(L+m_s-1) & \end{bmatrix}. \quad (2)$$

A code is said to be periodic with period T if $\mathbf{E}_\mu(t) = \mathbf{E}_\mu(t+T) \forall t \forall \mu = 0 \dots m_s$. The code's *constraint length* $\nu_s = N_s Q(m_s+1)$ corresponds to the maximal width of the support of the rows of the entire PCM $\mathbf{H}_{[0,L-1]} = \mathcal{L}\{\mathbf{E}_{[0,L-1]}\}$. With $(\cdot)^\top$ denoting the transpose operation,² a valid codeword \mathbf{c} comprises the concatenation of sub-codewords $\mathbf{c}(t) \in \mathbb{F}_2^{N_s Q \times 1}$ such that

$$\mathbf{c}^\top = [\mathbf{c}^\top(0), \dots, \mathbf{c}^\top(L-1)] \quad (3)$$

and fulfills (with the operators \oplus and \odot denoting addition and matrix-vector multiplication in \mathbb{F}_2 , respectively)

$$\bigoplus_{\mu=0}^{m_s} \mathbf{H}_\mu(t) \odot \mathbf{c}(t-\mu) = \mathbf{0} \quad \forall t \quad (4)$$

where $\mathbf{H}_\mu(t) = \mathcal{L}\{\mathbf{E}_\mu(t)\}$. In (4), handling of the termination is omitted for simplicity.

¹The term *exponent matrix* comes from an alternative representation of the rotation by using an appropriate rotation matrix, which is multiplied with itself E_{ji} times.

²Many coding theorists prefer row vectors over column vectors for codewords. Recent 3GPP releases however use column vectors for codewords, which is why we follow this way of notation.

2.1.3. Effects of the Termination

The top-most and bottom-most $m_s M_s$ CN blocks in $\mathbf{H}_{[0,L-1]}$ have smaller degrees than the ones in the middle of the PCM. This irregularity is the main reason for the excellent performance of SC-LDPC codes [16]. Since SC-LDPC codes exhibit recursive encoder structures, some effort is required to determine the termination sequence (given by the last sub-codewords in (3)) that fulfills the PC equations located at the bottom of the PCM [22]. By contrast, the fulfillment of the PC equations at the top of the PCM is trivially solved by initializing the encoder with an all-zero state.

Furthermore, termination reduces the code rate. Let L_u denote the number of coupling instants used to transmit user data (i.e., the information symbols) and L_t denote the number of coupling instants used for the termination sequence. Then $L = L_u + L_t$ and the length of the whole codeword is given by $n = LN_s Q$; the number of information symbols is given by $k = L_u(N_s - M_s)Q$. Hence, the effective code rate is

$$R_L = \frac{k}{n} = \frac{L_u(N_s - M_s)Q}{(L_u + L_t)N_s Q} = \frac{L_u}{L_u + L_t} R_\infty \quad (5)$$

with the asymptotic code rate

$$R_\infty = \lim_{L \rightarrow \infty} R_L = \frac{N_s - M_s}{N_s}. \quad (6)$$

2.1.4. Code Employed in This Paper

We use the QC code ensembles described in [23]. The codes are *asymptotically regular*, i.e., all VNs have the same degree d_v and all CNs the same degree d_c if the termination is not considered [17]. Such an ensemble is in short denoted as a (d_v, d_c) code ensemble. Theoretic analyses for these ensembles (albeit not requiring QC sub-matrices) such as decoding thresholds are available in, e.g., [16]. We focus on codes with $R_\infty = 1/2$, i.e., $d_c = 2d_v$. We use the smallest possible parameters to achieve that rate: $N_s = 2$, $M_s = 1$. In addition, we require fully populated matrices $\mathbf{E}_\mu(t)$ for all $\mu = 0 \dots m_s$ such that $m_s = d_v - 1$ since $M_s = 1$. The termination sequence comprises $L_t = m_s$ sub-codewords $\mathbf{c}(t)$ [22]. However, simulations are performed using only the all-zero codeword to avoid expensive matrix inversion. The codes are periodic with $T = 3$ such that reasonably large girths can be achieved according to the results in [23]. An ensemble is formed by independently and randomly choosing the cyclic shifts for each $\mathbf{E}_\mu(t)$ from a uniform distribution with support $[0, Q - 1]$ for each transmission. Finally, realizations where cycles of length 4 appear in the Tanner graph are excluded from the evaluation.

With respect to (3), the sub-codewords $\mathbf{c}(t) \in \mathbb{F}_2^{N_s Q \times 1}$ at each coupling instant $t = 0 \dots (L_u - 1)$ are formed in the following way (for $N_s = 2$ and $M_s = 1$, i.e., $N_s - M_s = 1$):

$$\mathbf{c}^\top(t) = \begin{bmatrix} \mathbf{b}^\top(t), \mathbf{p}^\top(t) \end{bmatrix}. \quad (7)$$

The $\mathbf{b}(t) \in \mathbb{F}_2^{Q \times 1}$ contain information symbols whereas the $\mathbf{p}(t) \in \mathbb{F}_2^{Q \times 1}$ contain parity symbols. In the termination sequence, the $\mathbf{c}(t)$ only consist of parity symbols. The concatenated vector

$$\mathbf{b}^\top = \begin{bmatrix} \mathbf{b}^\top(0), \dots, \mathbf{b}^\top(L_u - 1) \end{bmatrix} \quad (8)$$

then contains all k information symbols.

2.2. Message-Passing Decoding

Although SC-LDPC codes can be decoded like regular convolutional codes, i.e., with a Viterbi decoder, their large constraint lengths render such an approach infeasible [8]. Instead, the sparseness of the $\mathbf{H}_\mu(t)$ enables efficient iterative decoding with belief propagation [24]. The decoding output is given in the form of hard decisions that estimate the transmitted symbols from (7):

$$\hat{\mathbf{c}}^\top(t) = \begin{bmatrix} \hat{\mathbf{b}}^\top(t), \hat{\mathbf{p}}^\top(t) \end{bmatrix}. \quad (9)$$

For iterative decoding, the reliabilities of the n symbols of the complete received word \mathbf{y} are usually represented by Log-Likelihood Ratios (LLRs) with respect to the binary code symbols c_i , $i = 0 \dots (n - 1)$, to improve the numerical

stability of the iterative decoding process. Let (without loss of generality) the code symbol c_i be associated with a received symbol y . Then

$$L_{a,i} = \log \frac{\Pr\{C_i = 0 \mid Y\}}{\Pr\{C_i = 1 \mid Y\}} \quad (10)$$

represents the LLR given the received value where the random variables C_i and Y correspond to the realizations c_i and y , respectively. The updated reliabilities (incorporating extrinsic information) L_i for the n code symbols, i.e., $i = 0 \dots (n-1)$, are calculated at the VNs with

$$L_i = L_{a,i} + \sum_{j \in \mathcal{E}_c(i)} L_c(j \rightarrow i) \quad (11)$$

where $\mathcal{E}_c(i)$ is the set of CNs connected to VN i and $L_c(j \rightarrow i)$ is the message from CN j to VN i [25]. The message sent from VN i to CN j in the next iteration is given by

$$L_v(i \rightarrow j) = L_i - L_c(j \rightarrow i). \quad (12)$$

In the Sum-Product Algorithm (SPA), the CN messages are computed from $\mathcal{E}_v(j)$, the set of VNs connected to CN j , in an optimal way [25]:

$$\tanh\left(\frac{L_c(j \rightarrow i)}{2}\right) = \prod_{j \in \mathcal{E}_v(j) \setminus i} \tanh\left(\frac{L_v(i \rightarrow j)}{2}\right). \quad (13)$$

Equation (13) is prohibitively complex for implementation in practice. Therefore, approximations like the MSA are often applied [13]. In its simplest form, the MSA replaces (13) by

$$L_c(j \rightarrow i) = \prod_{j \in \mathcal{E}_v(j) \setminus i} \text{sign}\{L_v(i \rightarrow j)\} \cdot \min_{j \in \mathcal{E}_v(j) \setminus i} \{|L_v(i \rightarrow j)|\} \quad (14)$$

where the sign function is defined as

$$\text{sign}\{x\} = \begin{cases} 0 & \text{if } x = 0, \\ x/|x| & \text{otherwise.} \end{cases} \quad (15)$$

3. Windowed-Decoder Configurations Selected for Comparisons

We briefly introduce our notation for the WD and review the configurations relevant to the comparisons in this paper, i.e., window update strategies and PC-based Early Termination (ET).

3.1. Window Update Strategies

We need to strictly differentiate the *window update strategy*, i.e., how the definition of the decoding window affects VN and CN updates, from *update scheduling*, i.e., whether message updates are performed in a serial or parallel manner. In essence, two update strategies can be distinguished. For the first strategy—called the *VN-centered* strategy \mathcal{U}_{VN} from here on—a decoding window of size W is defined by the set of VNs for W consecutive sub-codewords $\mathbf{c}(t)$, cf. [4, 8, 9]. When QC codes as described above are used, the window thus consists of WN_s consecutive VN blocks, each of which consists of Q consecutive VNs. For the second strategy—called the *CN-centered* strategy \mathcal{U}_{CN} from here on—a decoding window of size W is defined by the set of WM_s consecutive CN blocks and all related VNs [5, 11].

Figure 1 depicts the decoding windows for both update strategies assuming an SC-LDPC code with memory $m_s = 2$. The shaded rectangles represent the structure of the exponent matrix $\mathbf{E}_{[0,L-1]}$: Each rectangle corresponds to one of the sub-matrices $\mathbf{E}_\mu(t)$ with M_s CN blocks and N_s VN blocks. Moving the window to the next position means shifting it down and right by one $\mathbf{E}_\mu(t)$ each, resulting in a large overlap between windows at two successive positions.

A decoding window with the VN-centered strategy \mathcal{U}_{VN} is indicated by the thick solid line; the contained sub-matrices are hatched in blue. Performing updates on VNs in the window still requires access to messages sent along

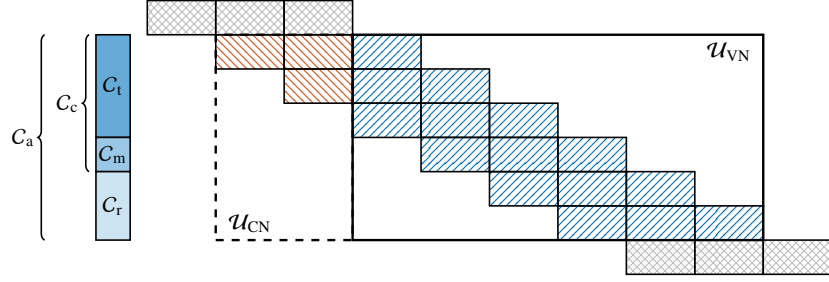


Figure 1: WD for $W = 6$ and a code with $m_s = 2$. The shaded rectangles represent the $E_\mu(t)$. The parts of the exponent matrix for which messages are updated with the VN-centered strategy \mathcal{U}_{VN} are contained within the thick solid line. With the CN-centered strategy \mathcal{U}_{CN} , the messages for the parts contained within the dashed line are updated as well.

edges related to the previous sub-matrices back-hatched in red, contained within the dashed line. However, those accesses are read-only. By contrast, the messages for both the blue and the red sub-matrices are updated with the CN-centered strategy \mathcal{U}_{CN} . In either case, messages along the edges corresponding to the sub-matrices outside the windows (crosshatched in gray) are not updated.

Please note that the method of amplifying LLR magnitudes for read-only messages in case of satisfied PC equations in previous window positions as proposed in [10] cannot be applied here. That is because we use serial update scheduling throughout this paper, which gives better results but is not compatible with the method of [10].

3.2. Parity-Based Early Termination and Window-Size Restrictions

With PC-based ET, the WD moves its decoding window from position w to position $w + 1$ if a certain number of iterations is completed or all selected PC equations are satisfied. We focus on the following sets of CNs indicated by the vertical bar at the left-hand side of Figure 1:

- C_t Target CNs; the top-most $M_s(m_s + 1)$ blocks of CNs in a decoding window. Closely related to the so-called target VNs that are no longer updated when the window moves to the next position.
- C_c Complete CNs; all CNs in a window except for the bottom-most $M_s m_s$ blocks of CNs. Only connected to VNs whose edges are completely covered by the decoding window. C_c consists of the target CNs C_t and the middle CNs C_m .
- C_a All CNs in a decoding window. C_a consists of the complete CNs C_c and the remaining CNs C_r .

Using the set C_a for ET is the most obvious approach as it corresponds to the procedure in block-code decoding. The authors of [10], however, propose using the set C_t .³ Using the set C_c , i.e., a choice in-between C_t and C_a , is proposed in [15].

For meaningful comparisons of the various sets of PC equations for ET, the window size W should be restricted such that $|C_t| < |C_c| < |C_a|$. In other words, we want to exclude the cases $|C_t| = |C_c|$ and $|C_c| = |C_a|$. Expressed in terms of code dimensions, these cardinalities are given by

$$|C_t| = (m_s + 1)M_s Q \quad (16)$$

$$|C_c| = (W - m_s)M_s Q \text{ and} \quad (17)$$

$$|C_a| = WM_s Q. \quad (18)$$

$|C_c| < |C_a|$ always holds for $m_s > 0$. To achieve $|C_t| < |C_c|$, we require

$$W > 2m_s + 1. \quad (19)$$

In general, the window size is kept small to maximize the reduction of internal memory compared to the Full Block Decoder (FBD), cf. the selected window sizes in [5, 9, 26], and others. However, a WD with a window size smaller

³The simplest choice, i.e., using only the top-most M_s blocks of PC equations in the window, would result in a poor decoding performance for $M_s = 1$ as is used in this paper.

than a certain minimal size may have a larger iterative decoding threshold than the FBD [16]. We still include small window sizes in our evaluations to highlight the effects of nonideal implementations, e.g., caused by fixed-point calculations.

4. Transmission Setup and Decoder Parameters to Achieve Equal Maximal Complexity

The simulation setup and the parameters used to achieve equal maximal computational complexity are given in this section.

4.1. Transmission Parameters

For the simulation results presented below, the (5,10) ensemble as described in Section 2 is used. The lifting factor is set to $Q = 256$ and the coupling length is $L = 100$, giving a codeword length of $n = 51200$. The resulting code rate is $R = 0.48$, i.e., the rate reduction is 4% compared to the asymptotic code rate of $R_\infty = 1/2$. As mentioned above, simulations are performed using only the all-zero codeword. The code symbols are modulated using 16-ary Quadrature Amplitude Modulation (QAM) with Gray mapping to match the rate proposed for 5G NR as given in [27]; such a setup is also used in [28]. The code symbols are used in sequence without interleaving before the QAM mapping. Scrambling as described in [29] is used such that the complex-valued QAM symbols are uniformly distributed over the whole QAM constellation.

A fading channel with Additive White Gaussian Noise (AWGN) is used to simulate transmissions in a typical wireless communication system. The statistical model is taken from [30] as this model accords well with today's communication systems, e.g., Wi-Fi or 5G NR. It accounts for the use of Orthogonal Frequency-Division Multiplexing (OFDM) in conjunction with Multiple-Input Multiple-Output (MIMO) transmissions. The channel is modeled by Maximum-Ratio Combining (MRC) of 4 independent propagation paths, each exhibiting Rayleigh fading. This channel setup corresponds to, e.g., 2×2 MIMO-OFDM with appropriate Space-Frequency Block Coding (SFBC) [31] and ideal Channel State Information (CSI) at the receiver. With sufficient interleaving in frequency, the fading coefficients are independent and identically distributed (i.i.d.) for each QAM symbol. The mean Signal-to-Noise Ratio (SNR) is indicated by E_s/N_0 where E_s is the average energy per QAM symbol and N_0 is the one-sided noise Power Spectral Density (PSD).

4.2. General Decoder Configuration

All decoders in this paper implement the decoding algorithm from [32] using fixed-point arithmetic with an LLR-magnitude resolution of 10 bit. This decoding algorithm is a blend of the accurate SPA and the approximate MSA: When processing a CN, only the outgoing message sent along the edge with the weakest incoming message is computed accurately with the SPA; the combination of *all* incoming messages with appropriate signs (again with the SPA) is used for all other outgoing messages.

Furthermore, row-wise serial layered scheduling as described in [12] is applied. With QC codes and assuming $M_s = 1$, the Q PC equations formed by one row in $E_{[0,L-1]}$ are orthogonal to each other, which is why the respective CN updates can be processed in parallel without numerical dependencies. One such row is denoted as a *layer*. Thus, the l -th layer \mathcal{L}_l consists of the following block of Q consecutive CNs:

$$\mathcal{L}_l = \{lQ, lQ + 1, \dots, (l+1)Q - 1\}. \quad (20)$$

Serial scheduling means that the outgoing messages are updated for one layer at a time and the related symbol reliabilities are updated before updating the next layer. This procedure stands in contrast to *parallel* update schedules where the messages are updated for all layers before the symbol reliabilities are updated. In our WD implementation, the layers within each window are updated from top to bottom with respect to the exponent matrix $E_{[0,L-1]}$ from (2).

For consistency, a decoding window of size W is assumed to always contain W layers when $M_s = 1$. In other words, the top layer in the first window is the top row of the exponent matrix; the bottom layer in the last window is the bottom row of the exponent matrix. Thus, there are

$$Q = L + m_s - W + 1 \quad (21)$$

unique window positions and the window virtually extends beyond the left-hand or right-hand sides of $E_{[0,L-1]}$ during the first and last m_s positions. These positions contain the CNs with reduced degrees. Formally, a window of size W at position w , $w = 0 \dots (\Omega - 1)$, is defined as the set of all layers that are updated:

$$\mathcal{W}_W^{(w)} = \{\mathcal{L}_l : w \leq l < w + W\}. \quad (22)$$

4.3. Achieving Equal Maximal Complexity

A WD using the VN-centered update strategy \mathcal{U}_{VN} disregards message updates for the edges back-hatched in red in Figure 1. The key principle in this paper is to consider this difference in the number of message updates when aiming for equal overall computational complexity for all configurations. To be precise, we measure the complexity in terms of the number of message updates (with respect to the exponent matrix) to decode all k information symbols. A similar principle is applied in [33] to evaluate infinitely long, nonterminated codes. To our best knowledge, comparisons of different decoder configurations with finite-length codes, however, have not yet been proposed.

The upper limit on the decoding complexity is given by a Full Block Decoder (FBD), i.e., a decoder with $W = L + m_s$, performing up to $\Lambda_{\text{max,FBD}} = 200$ iterations. We could not find significant improvements in the decoding performance with additional iterations. The WD performs an appropriate maximal number of iterations *per window* such that the total maximal number of message updates I_{max} does not surpass that of the FBD. From here on, all quantities regarding the number of message updates relates to the code's exponent matrix, i.e., the lifting factor Q is ignored.

Formally, let $I_{1,\text{FBD}}$ denote the number of message updates with a single iteration with the FBD (which equals the number of edges in the Tanner graph):

$$I_{1,\text{FBD}} = \sum_{j=0}^{M-1} |\mathcal{E}_v(j)| \quad (23)$$

where M is the number of rows in $E_{[0,L-1]}$. For a WD with the CN-centered update strategy \mathcal{U}_{CN} , the number of message updates with a single iteration in each window is

$$I_{1,\text{WD}}^{\text{C}}(W) = \sum_{w=0}^{\Omega-1} \sum_{j \in \mathcal{W}_W^{(w)}} |\mathcal{E}_v(j)| \quad (24)$$

whereas with the VN-centered strategy \mathcal{U}_{VN} it is

$$I_{1,\text{WD}}^{\text{V}}(W) = \sum_{w=0}^{\Omega-1} \sum_{j \in \mathcal{W}_W^{(w)}} |\mathcal{E}_v(j) \setminus \mathcal{V}_e^{(w)}| \quad (25)$$

where $\mathcal{V}_e^{(w)}$ denotes the VNs not updated at position w .

Finally, the maximal computational effort $\Lambda_{\text{max,FBD}} I_{1,\text{FBD}}$, i.e., the number of message updates when the FBD performs $\Lambda_{\text{max,FBD}}$ iterations, is converted to a maximal number of iterations per window $\Lambda_{\text{max,WD}}(W)$ for the WD:

$$\Lambda_{\text{max,WD}}(W) = \left\lfloor \Lambda_{\text{max,FBD}} \frac{I_{1,\text{FBD}}}{I_{1,\text{WD}}(W)} \right\rfloor \quad (26)$$

where $\lfloor \cdot \rfloor$ is the floor operation.

From here on, we omit subscripts and arguments related to the number of iterations or the number of message updates for brevity. Table 1 lists the maximal number of iterations (per window) Λ_{max} and the corresponding maximal number of message updates $I_{\text{max}} = \Lambda_{\text{max}} I_1$ for all configurations used throughout this paper. The largest relative difference in I_{max} to the value targeted with the FBD is about 5% due to rounding, which we consider small enough.

Instead of comparing \mathcal{U}_{VN} and \mathcal{U}_{CN} for the same window size and allowing different values for Λ_{max} , we choose different window sizes such that the number of message updates per window per iteration (described by N_m in Table 1)

Decoder	W	N_m	Λ_{\max}	I_{\max}
FBD	–		200	200 000
WD, \mathcal{U}_{VN}	12	100	21	194 460
	14	120	18	195 840
	16	140	16	198 720
	20	180	13	198 380
WD, \mathcal{U}_{CN}	10	100	21	197 820
	12	120	18	199 440
	14	140	15	189 900

Table 1: Number of message updates per window per iteration (N_m), maximal number of iterations per window (Λ_{\max}), and maximal number of message updates with Λ_{\max} iterations per window (I_{\max}).

is roughly the same for both configurations.⁴ Even though the match is not always perfect, a WD using \mathcal{U}_{CN} with a window of size W is compared to a WD using \mathcal{U}_{VN} with a window of size $W + 2$ in our simulations presented in Section 5.

4.4. Metrics for Evaluation

The decoding performance is evaluated by means of the *Block Error Ratio* (BLER) (cf. (7)–(9))

$$P_c := \Pr\{\hat{\mathbf{b}} \neq \mathbf{b}\} \quad (27)$$

and the *Average Number of Message Updates* (ANMU) \bar{I} with respect to the exponent matrix. With Early Termination (ET), $\bar{I} \leq I_{\max}$. Due to the differences in I_{\max} across different configurations, we evaluate the ratio

$$\bar{t} := \frac{\bar{I}}{I_{\max}} \quad (28)$$

and refer to \bar{t} as the *relative* ANMU.

5. Joint Evaluation of Early Termination and Update Strategies

The numerical results in this section have been obtained from 10^6 realizations of the channel and the code ensemble each, i.e., a new code realization and a new channel realization have been generated for each new transmission. The simulation setup is described in Section 4. Our aim is to determine the configuration for a WD with the smallest resulting average computational complexity without sacrificing the decoding performance too much. We jointly consider Early Termination (ET) based on PC equations, different window update strategies, and various window sizes W as discussed in Section 3. To keep the evaluation organized, we first present results for varying window sizes W and various sets of PC equations for ET using only the VN-centered update strategy \mathcal{U}_{VN} . Afterwards, we present a comparison of \mathcal{U}_{VN} against the CN-centered update strategy \mathcal{U}_{CN} . In all cases, the maximal number of iterations per window was adjusted for equal maximal complexity according to Table 1. The results for a Full Block Decoder (FBD) are given for reference.

5.1. Impact of the Window Size and Early Termination

For the first part of this evaluation, we selected the CN sets C_c (complete CNs) and C_t (target CNs) for ET. The CN set C_a (all CNs) was excluded since PC equations at the bottom of a window are expected to almost never be satisfied. That is because the Bit Error Ratios (BERs) of the right-most VNs in the window are close to 1 [9]. We selected window sizes $W \in \{12, 16, 20\}$ to satisfy the constraint given by (19) and to get an overview of larger windows as well.

⁴The values for N_m assume a single decoding window in the middle of the exponent matrix. By contrast, the remaining values in Table 1 assume a terminated code with $L = 100$ as described above.

Figure 2 portrays the relative Average Number of Message Updates (ANMU) $\bar{\iota}$ from (28) over the SNR E_s/N_0 . Only considering the PC equations in C_t for ET reduces $\bar{\iota}$ compared to considering the PC equations in C_c . The top-most PC equations in a window are formed by more reliable VNs. In addition, the smaller number of PC equations in C_t can become satisfied more quickly. Depending on the SNR, $\bar{\iota}$ is reduced by up to 49% with $W = 12$; up to 58% with $W = 16$, and by up to 60% with $W = 20$ when selecting the set C_t instead of C_c for ET. Moreover, any WD evaluated here converges faster than the FBD except when considering the domain of very high SNR.

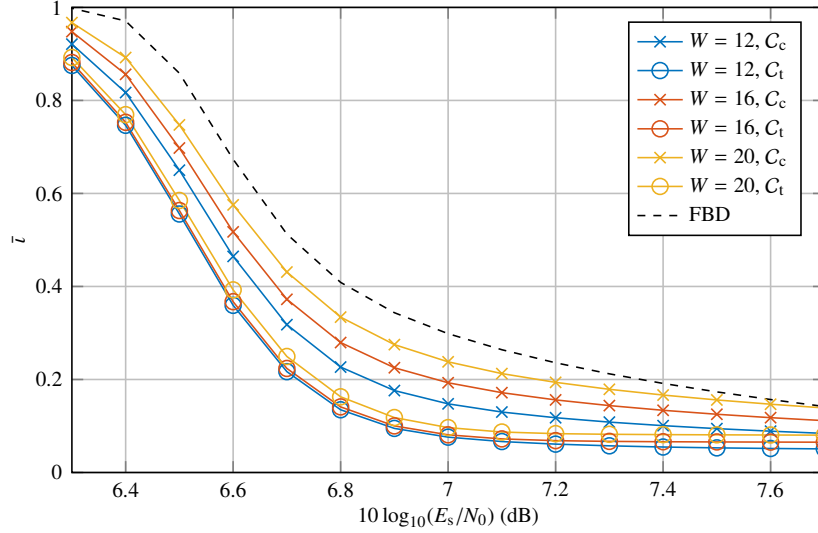


Figure 2: Relative ANMU $\bar{\iota}$ over the SNR E_s/N_0 with various sets of PC equations for ET and various window sizes W using the update strategy \mathcal{U}_{VN} .

The window size W also influences $\bar{\iota}$: When selecting the PC equations in C_c for ET, choosing smaller windows results in faster convergence than choosing larger windows. Since $|C_c|$ grows with the window size, larger windows require more PC equations to be satisfied. This, in turn, requires a greater amount of message updates. When choosing C_t for ET, however, the differences between smaller and larger window sizes are much smaller because $|C_t|$ is independent of W . In this case, a large window may actually *increase* the decoding complexity because more messages are updated in each iteration. This effect is especially visible in the domain of high SNR where usually a single iteration per window is sufficient to satisfy the PC equations in C_t .

The decoding performance as measured by the Block Error Ratio (BLER) P_c from (27) is mostly determined by the window size W . As shown in Figure 3, using larger windows results in fewer residual errors because of the simplified transport of information across the whole Tanner graph. At a working point of $P_c = 10^{-2}$, the gap in the SNR to the FBD constitutes around 0.25 dB with any W . The gap increases with increasing SNR where the largest gap can be observed for $W = 12$; the differences between the decoders with $W = 16$ and $W = 20$ are negligible. Interestingly, the choice of PC equations for ET only has a minor impact on P_c : Using the smaller set C_t results in about the same (or even a smaller) number of residual decoding errors as using the larger set C_c . Thus, the smaller number of PC equations in C_t seems sufficient to verify the estimates of the sub-codewords in the decoding window.

Furthermore, the error floor is relatively high—even for the FBD. Despite the omission of code realizations with cycles of length 4 in the Tanner graph, the employed code ensemble does not perform well in general. The WD’s error floor is even higher than the FBD’s since the WD can easily get stuck and propagate errors due to the unidirectional decoding. Nonetheless, our main concern is the gap in the SNR at $P_c = 10^{-2}$, which is a typical working point in cellular systems [34].

Summing up, ET based on PC equations works very well. The set C_t represents the best choice for ET in all considered aspects as a very low computational complexity can be achieved this way. Additionally, a WD with a surprisingly large window size of, e.g., $W = 16$ seems to be an overall good choice as it practically matches the decoding performance of a WD with $W = 20$ while offering a reduced computational complexity.

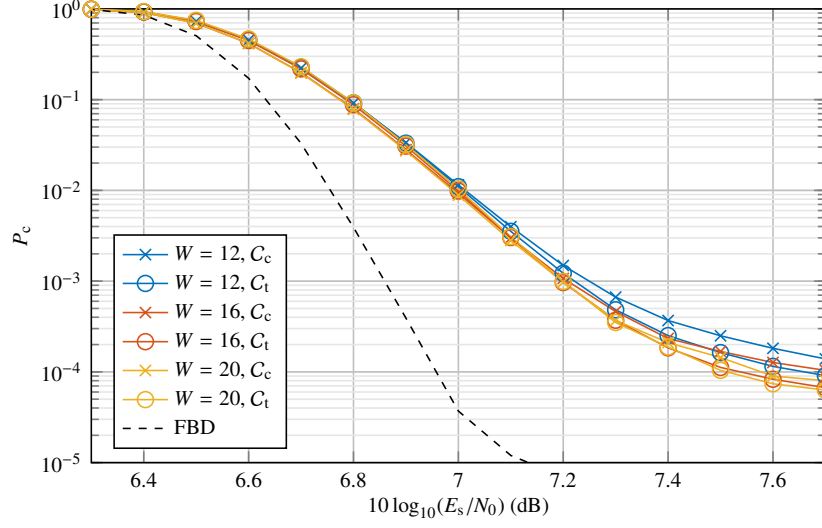


Figure 3: BLER P_c over the SNR E_s/N_0 with various sets of PC equations and various window sizes W using the update strategy \mathcal{U}_{VN} .

5.2. Comparison of Update Strategies

For the second part of this evaluation, we compared the two window update strategies reviewed in Section 3. Specifically, we compared a WD using \mathcal{U}_{CN} with window size W against a WD using \mathcal{U}_{VN} with window size $W + 2$ as argued in Section 4. Furthermore, we selected $W \in \{12, 14, 16\}$ for \mathcal{U}_{VN} and thus $W \in \{10, 12, 14\}$ for \mathcal{U}_{CN} as larger windows did not significantly improve the decoding performance, cf. Figure 3. Following our findings from the evaluations above, we solely considered the CN set C_t for ET.

Figure 4 depicts the relative ANMU $\bar{\tau}$ for the configurations listed above. Using \mathcal{U}_{CN} with $W = 10$ results in the worst decoding complexity. All other configurations perform slightly better with only small differences among them. Using \mathcal{U}_{VN} results in minor advantages over using \mathcal{U}_{CN} . As before, all WD configurations beat the FBD in terms of computational complexity.

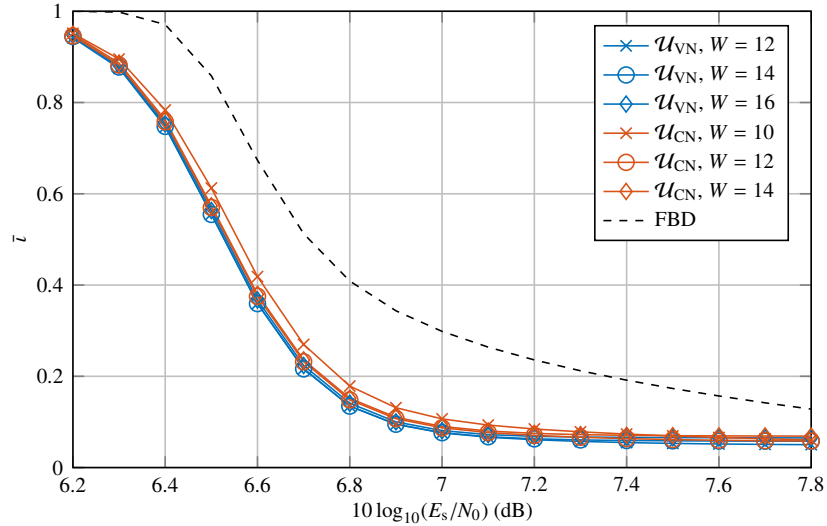


Figure 4: Relative ANMU over the SNR E_s/N_0 comparing \mathcal{U}_{CN} with $W \in \{10, 12, 14\}$ against \mathcal{U}_{VN} with $W \in \{12, 14, 16\}$. The PC equations in C_t are used for ET.

The BLER P_c is shown in Figure 5. According with the results from Figure 3, the window size W is the most decisive factor for the resulting decoding performance. Still, the differences between using \mathcal{U}_{VN} with window size $W + 2$ and using \mathcal{U}_{CN} with window size W are negligible. Thus, the comparison with a normalized per-window complexity can indeed be considered to be fair.

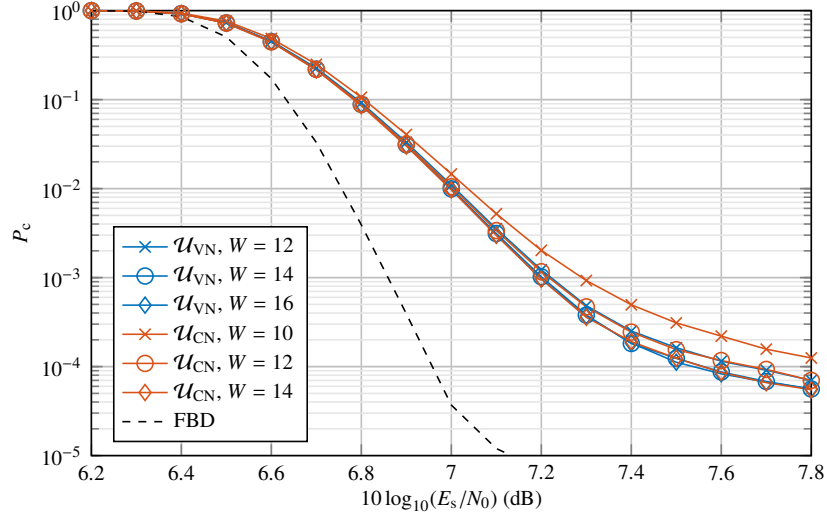


Figure 5: BLER over the SNR E_s/N_0 comparing \mathcal{U}_{CN} with $W \in \{10, 12, 14\}$ against \mathcal{U}_{VN} with $W \in \{12, 14, 16\}$. The PC equations in C_t are used for ET.

Summing up the whole evaluation, using only the PC equations corresponding to the CNs in C_t is the superior choice for minimizing the computational complexity. The computational complexity is then reduced when using a medium window size (e.g., $W = 16$) rather than smaller or larger window sizes. Furthermore, the VN-centered update strategy \mathcal{U}_{VN} is the overall better update strategy: The computational complexity is improved while the decoding performance is kept at a similar level as a window of size $W + 2$ can be used in a fair comparison against \mathcal{U}_{CN} with window size W . The only downside of using \mathcal{U}_{VN} is the more challenging implementation in conjunction with CN-wise serial scheduling and the Min-Sum Algorithm (MSA) since not all messages for all the CNs in the decoding window are updated.

6. Conclusion

Limiting a Windowed Decoder (WD) for SC-LDPC codes to the same maximal decoding complexity as a Full Block Decoder (FBD) reveals the following results: It is only possible to beat the FBD in terms of computational complexity with an optimized configuration. With the configuration derived in this paper, the resulting WD requires on average only half the decoding complexity of the FBD while simultaneously showing a gap in the SNR of only around 0.25 dB for a working point with BLER $P_c = 10^{-2}$. Comparison of various update strategies shows that it may be advantageous to skip updates of some messages in the decoding window. The window can then be enlarged to achieve the same computational complexity while improving the decoding performance. Lastly, all results obtained in this paper have been achieved with configurations requiring low control overhead, making the proposed WD design very suitable for efficient hardware implementation.

References

- [1] A. Jimenez Feltström, K. S. Zigangirov, Time-varying periodic convolutional codes with low-density parity-check matrix, *IEEE Trans. Inf. Theory* 45 (6) (1999) 2181–2191.
- [2] R. Tanner, D. Sridhara, A. Sridharan, T. Fuja, D. J. Costello, LDPC block and convolutional codes based on circulant matrices, *IEEE Trans. Inf. Theory* 50 (12) (2004) 2966–2984.

- [3] S. Kudekar, T. Richardson, R. L. Urbanke, Spatially coupled ensembles universally achieve capacity under belief propagation, *IEEE Trans. Inf. Theory* 59 (12) (2013) 7761–7813.
- [4] A. Pusane, A. Feltström, A. Sridharan, M. Lentmaier, K. Zigangirov, D. J. Costello, Implementation aspects of LDPC convolutional codes, *IEEE Trans. Commun.* 56 (7) (2008) 1060–1069.
- [5] A. R. Iyengar, M. Papaleo, P. H. Siegel, J. K. Wolf, A. Vanelli-Coralli, G. E. Corazza, Windowed decoding of protograph-based LDPC convolutional codes over erasure channels, *IEEE Trans. Inf. Theory* 58 (4) (2012) 2303–2320.
- [6] S. Abu-Surra, E. Pisek, R. Taori, Spatially-coupled low-density parity check codes: Zigzag-window decoding and code-family design considerations, in: *Proc. 2015 IEEE Inf. Theory Appl. Work. (ITA)*, San Diego, CA, USA, 2015, pp. 275–281.
- [7] K. Klaiber, S. Cammerer, L. Schmalen, S. ten Brink, Avoiding burst-like error patterns in windowed decoding of spatially coupled LDPC codes, in: *Proc. 10th IEEE Int. Symp. Turbo Codes Iterative Inf. Process. (ISTC 2018)*, Hong Kong, Hong Kong, 2018, pp. 1–5.
- [8] M. Papaleo, A. R. Iyengar, P. H. Siegel, J. K. Wolf, G. E. Corazza, Windowed erasure decoding of LDPC convolutional codes, in: *Proc. 2010 IEEE Inf. Theory Work. (ITW)*, Cairo, Egypt, 2010, pp. 1–5.
- [9] N. Ul Hassan, A. E. Pusane, M. Lentmaier, G. P. Fettweis, D. J. Costello, Non-uniform window decoding schedules for spatially coupled LDPC codes, *IEEE Trans. Commun.* 65 (2) (2017) 501–510.
- [10] I. Ali, J.-H. Kim, S.-H. Kim, H. Kwak, J.-S. No, Improving windowed decoding of SC LDPC codes by effective decoding termination, message reuse, and amplification, *IEEE Access* 6 (2017) 9336–9346.
- [11] A. Beemer, C. A. Kelley, Avoiding trapping sets in SC-LDPC codes under windowed decoding, in: *Proc. 2016 Int. Symp. Inf. Theory Appl. (ISITA)*, Monterey, CA, USA, 2016, pp. 206–210.
- [12] E. Yeo, P. Pakzad, B. Nikolic, V. Anantharam, High throughput low-density parity-check decoder architectures, in: *Proc. 2001 IEEE Global Commun. Conf. (GLOBECOM)*, San Antonio, TX, USA, 2001, pp. 3019–3024.
- [13] M. Fossorier, M. Mihaljevic, H. Imai, Reduced complexity iterative decoding of low-density parity check codes based on belief propagation, *IEEE Trans. Commun.* 47 (5) (1999) 673–680.
- [14] S. Mo, L. Chen, Improved sliding window decoding of spatially coupled low-density parity-check codes, in: *Proc. 2017 IEEE Inf. Theory Work. (ITW)*, Kaohsiung, Taiwan, 2017, pp. 126–130.
- [15] P. Kang, Y. Xie, L. Yang, J. Yuan, Reliability-based windowed decoding for spatially-coupled LDPC codes, *IEEE Commun. Lett.* 7798 (1089) (2018) 1322–1325.
- [16] M. Lentmaier, A. Sridharan, D. J. Costello, K. S. Zigangirov, Iterative decoding threshold analysis for LDPC convolutional codes, *IEEE Trans. Inf. Theory* 56 (10) (2010) 5274–5289.
- [17] D. Mitchell, R. Smarandache, M. Lentmaier, D. J. Costello, Quasi-cyclic asymptotically regular LDPC codes, in: *Proc. 2010 IEEE Inf. Theory Work. (ITW)*, IEEE, Dublin, Ireland, 2010, pp. 1–5.
- [18] Y. Kou, S. Lin, M. P. C. Fossorier, Low-density parity-check codes based on finite geometries: a rediscovery and new results, *IEEE Trans. Inf. Theory* 47 (7) (2001) 2711–2736.
- [19] 3GPP, Technical Specification Group Radio Access Network; NR; Multiplexing and Channel Coding (Release 15), TS 38.212, V15.8.0 (Dec. 2019).
- [20] J. Thorpe, Low-density parity-check (LDPC) codes constructed from protographs, *Interplanetary Network Progress Report* 154 (2003) 1–7.
- [21] Seho Myung, Kyeongcheol Yang, Youngkyun Kim, Lifting methods for quasi-cyclic LDPC codes, *IEEE Commun. Lett.* 10 (6) (2006) 489–491.
- [22] Z. Chen, T. L. Brandon, S. Bates, D. G. Elliott, B. F. Cockburn, Efficient implementation of low-density parity-check convolutional code encoders with built-in termination, *IEEE Trans. Circuits Syst. I* 55 (11) (2008) 3628–3640.
- [23] V. A. Chandrasekty, S. J. Johnson, G. Lechner, Memory-efficient quasi-cyclic spatially coupled low-density parity-check and repeat-accumulate codes, *IET Commun.* 8 (17) (2014) 3179–3188.
- [24] D. MacKay, Good error-correcting codes based on very sparse matrices, *IEEE Trans. Inf. Theory* 45 (2) (1999) 399–431.
- [25] J. Hagenauer, E. Offer, L. Papke, Iterative decoding of binary block and convolutional codes, *IEEE Trans. Inf. Theory* 42 (2) (1996) 429–445.
- [26] M. Lentmaier, M. M. Prenda, G. P. Fettweis, Efficient message passing scheduling for terminated LDPC convolutional codes, in: *Proc. 2011 IEEE Int. Symp. Inf. Theory (ISIT)*, St. Petersburg, Russia, 2011, pp. 1826–1830.
- [27] 3GPP, Technical Specification Group Radio Access Network; NR; Physical Layer Procedures for Data (Release 15), TS 38.214, V15.8.0 (Dec. 2019).
- [28] L. Schmalen, S. Ten Brink, Combining spatially coupled LDPC codes with modulation and detection, in: *Proc. 9th Int. ITG Conf. Syst. Commun. Coding (SCC 2013)*, Munich, Germany, 2013.
- [29] 3GPP, Technical Specification Group Radio Access Network; NR; Physical Channels and Modulation (Release 15), TS 38.211, V15.8.0 (Dec. 2019).
- [30] S. Müller-Weinfurter, Coding approaches for multiple antenna transmission in fast fading and OFDM, *IEEE Trans. Signal Process.* 50 (10) (2002) 2442–2450.
- [31] D. Tse, P. Viswanath, *Fundamentals of Wireless Communication*, Cambridge University Press, Cambridge, UK, 2005.
- [32] C. Jones, E. Vallés, M. Smith, J. Villasenor, Approximate-min* constraint node updating for LDPC code decoding, in: *Proc. 2003 IEEE Military Commun. Conf. (MILCOM)*, Boston, MA, USA, 2003, pp. 157–162.
- [33] M. Battaglioni, M. Baldi, E. Paolini, Complexity-constrained spatially coupled LDPC codes based on protographs, in: *Proc. 2017 IEEE Int. Symp. Wirel. Commun. Syst. (ISWCS)*, Bologna, Italy, 2017, pp. 49–53.
- [34] 3GPP, Technical Specification Group Radio Access Network; NR; User Equipment (UE) radio transmission and reception; Part 1: Range 1 Standalone (Release 15), TS 38.101-1, V15.8.2 (Dec. 2019).